Research Article

Automated detection of the yellow-legged hornet (*Vespa velutina*) using an optical sensor with machine learning

Cayetano Herrera,[a] Mark Williams,[b] Joao Encarnação,[b]
Núria Roura-Pascual,[c] Bastian Faulhaber,[b] José Antonio Jurado-Rivera[d*]
and Mar Leza[a]

Abstract

BACKGROUND: The yellow-legged hornet (*Vespa velutina*) is native to Southeast Asia and is an invasive alien species of concern in many countries. More effective management of populations of *V. velutina* could be achieved through more widespread and intensive monitoring in the field, however current methods are labor intensive and costly. To address this issue, we have assessed the performance of an optical sensor combined with a machine learning model to classify *V. velutina* and native wasps/hornets and bees. Our aim is to use the results of the present work as a step towards the development of a monitoring solution for *V. velutina* in the field.

RESULTS: We recorded a total 935 flights from three bee species: *Apis mellifera, Bombus terrestris* and *Osmia bicornis;* and four wasp/hornet species: *Polistes dominula, Vespula germanica, Vespa crabro* and *V. velutina*. The machine learning model achieved an average accuracy for species classification of $80.1 \pm 13.9\%$ and $74.5 \pm 7.0\%$ for *V. velutina. V. crabro* had the highest level of misclassification, confused mainly with *V. velutina* and *P. dominula*. These results were obtained using a 14-value peak and valley feature derived from the wingbeat power spectral density.

CONCLUSION: This study demonstrates that the wingbeat recordings from a flying insect sensor can be used with machine learning methods to differentiate *V. velutina* from six other Hymenoptera species in the laboratory and this knowledge could be used to help develop a tool for use in integrated invasive alien species management programs.
© 2022 The Authors. *Pest Management Science* published by John Wiley & Sons Ltd on behalf of Society of Chemical Industry.

Supporting information may be found in the online version of this article.

Keywords: automated detection; Hymenoptera; pest management; *vespa velutina*; wingbeat frequency

1 INTRODUCTION

The yellow-legged hornet *Vespa velutina* Lepeletier, 1836 is an invasive alien species accidentally introduced in Europe from Asia in 2004.[1] For the affected regions, the control of *V. velutina* represents both an economic cost,[2,3] and an ecological impact whose full extent is still being investigated.[4,5] The monitoring of populations of *V. velutina* can assist the management of incursions and provide a better understanding of the spatio-temporal patterns of the species.[6]

The population distribution and dynamics of *V. velutina* are currently assessed through the trapping of adults[7,8] or by nest location[8] although these approaches are labor intensive, and trapping can have a negative impact on non-target insects.[9,10] Various automated methods are being trialed to monitor *V. velutina*, including radiotelemetry,[11] harmonic radar,[12] thermal imaging[13] and drones.[14]

In general terms, a wide range of methods is available to monitor biological diversity, such as: analysis of environmental DNA[15]

or RNA from terrestrial hematophagous parasites,[16] remote sensing[17] or citizen science projects.[8,18] Automated monitoring approaches using sensors have the potential to be more cost effective and provide more timely results than existing manual

* Correspondence to: JA Jurado-Rivera, Department of Biology (Genetics), University of the Balearic Islands, Ctra. Valldemossa km 7.5, Palma, Illes Balears, Spain. E-mail: jose.jurado@uib.es

a Department of Biology (Zoology), University of the Balearic Islands, Palma, Spain

b Irideon S.L., Barcelona, Spain

c Departament de Ciències Ambientals, Universitat de Girona, Girona, Spain

d Department of Biology (Genetics), University of the Balearic Islands, Palma, Spain

or laboratory methods and could also be used to complement existing methods.

Acoustic and vibrational-based methods are an important tool for monitoring biodiversity[19,20] and might also be used to monitor *V. velutina*. The approach generally uses a digital recorder in the field to collect animal sounds that are species specific, to derive estimates of species abundance and diversity at spatial and temporal scales.[20,21] Acoustic technology has been used in studies of marine mammals,[22] birds,[23] frogs[24] and insects.[25–27] In many cases, remote monitoring of animal sounds can outperform skilled observers.[28] It has also been used to monitor invasive alien species, such as red-billed leiothrix *Leiothrix lutea* (Scopoli, 1786),[29] cane toad *Bufo marinus* (Linnaeus, 1758),[30] coconut rhinoceros beetle *Oryctes rhinoceros* (Linnaeus, 1758),[31] red palm weevil *Rhynchophorus ferrugineus* (Olivier, 1791)[32] and tiger mosquito *Aedes albopictus* (Skuse, 1894).[33]

In the case of flying insects which emit a sound as they fly, acoustic methods are often used to determine the insect wingbeat frequency, since wingbeat frequency can be species specific.[20] However, it can be difficult to obtain acceptable quality audio recordings of free flying insects in the field due to the presence of background noise[34,35] and where swarms of insects are present.

To address the limitations of acoustic methods, optical methods have been used in which a light source and a light sensor are used to illuminate an individual flying insect and to detect the light reflected and scattered, or attenuated, by the insect in flight.[36–38] Under similar conditions, the fundamental wingbeat frequency reported by an optical sensor and by an acoustic sensor should be similar when both sensors are designed to detect the wingbeat of the flying insect.

Our study is designed to assess the hypothesis that the flights of *V. velutina* may be automatically differentiated from the flights of other Hymenoptera species based on features derived from the wingbeat recordings of a flying insect sensor. The other Hymenoptera species are: *Apis mellifera* Linnaeus, 1758, *Bombus terrestris* (Linnaeus, 1758), *Osmia bicornis* (Linnaeus, 1758); *Polistes dominula* (Christ, 1791), *Vespula germanica* (Fabricius, 1793) and *Vespa crabro* Linnaeus, 1758 which are likely to coexist in the field with the invasive *V. velutina*. Our overall aim is to contribute to the development of an automatic system to monitor populations of *V. velutina* in the field.

2 MATERIAL AND METHODS

2.1 Data collection

Individuals from seven Hymenopteran species were collected in the field: three bee species (*A. mellifera*, *B. terrestris* and *O. bicornis*) and four wasp/hornet species (*P. dominula*, *V. germanica*, *V. crabro* and *V. velutina*) as shown in Table 1.

The insects were collected during 2019 and 2022 in the Balearic Islands and Catalonia, Spain. For the six social Hymenoptera species, only individuals of the worker caste were collected because it is the most populous caste and the one whose members are most likely to be found outside the nest. For the solitary Hymenoptera species (*O. bicornis*) only males were collected because they are more abundant than females during breeding season. The insects were carefully collected and transported to the laboratory in an entomological tent ($25 \times 25 \times 25$ cm) in less than 1 h.

In the laboratory, individuals were transferred to a larger entomological tent ($60 \times 60 \times 60$ cm), after rejecting any insects with signs of damage to their body or wings. The tent contained a flying insect optical sensor developed by Irideon S.L. (Barcelona, Spain) which automatically recorded the wingbeat waveform of each insect as it flew through the sensor (Fig. 1(A)). For practical reasons, all individuals of the same species were introduced into the tent at a time, so each individual could give rise to zero, one, or more than one recording per session. *Vespa velutina* and *V. crabro* were each recorded in two separate sessions, but each individual was used in one recording session only. Each recording session lasted about 1 h and was ended when all individuals in the tent had stopped flying.

The sensor contained an optical emitter panel and an optical receiver panel, which faced each other across a distance of 19.7 cm, through which insects could fly. The optical emitter comprised a two-dimensional (2D) array of 940 nm wavelength infrared light emitting diodes (LEDs), and the optical receiver comprised a 2D array of 940 nm photodiodes. The emitter and receiver panels each had an active area of 10.2×7.1 cm. The volume of space bounded by the emitter and receiver panels was equal to $10.2 \times 7.1 \times 19.4$ cm (or 1405 cm^3) and is referred to as the sensing volume. The sensor had the following design attributes: a well-defined sensing volume with a relatively even response to an insect flying anywhere within the sensing volume, negligible sensitivity to insects flying outside of the sensing volume, and good immunity to background acoustic noise. The basic operating principle of the optical sensor is illustrated in Fig. 1(B). Further details about the sensor technology can be found in the references[39, 40].

The analog output signal of the optical sensor was acquired by an analog to digital converter (ADC) to digitize the signal. When a flying insect entered the sensing volume, it automatically triggered a single recording of 106.7 milliseconds in duration, comprising 1024 discrete ADC samples taken at a rate of 9603 samples per second. The duration of each

Table 1. Main characteristics of the seven Hymenopteran species used in this study, including the number of insects collected and the number of recordings made for each species

|	Species	Sex	Caste	No. individuals	No. flight records	Date of collection
Bees	*Apis mellifera*	Female	Worker	126	178	24-11-2021
	Bombus terrestris	Female	Worker	11	121	26-02-2019
	Osmia bicornis	Male	-	79	120	23-02-2021
Wasps/Hornets	*Polistes dominula*	Female	Worker	42	108	10-02-2020
	Vespa crabro	Female	Worker	10	91	20-10-2021
	Vespa velutina	Female	Worker	30	117	11-10-2021
	Vespula germanica	Female	Worker	22	200	09-10-2019
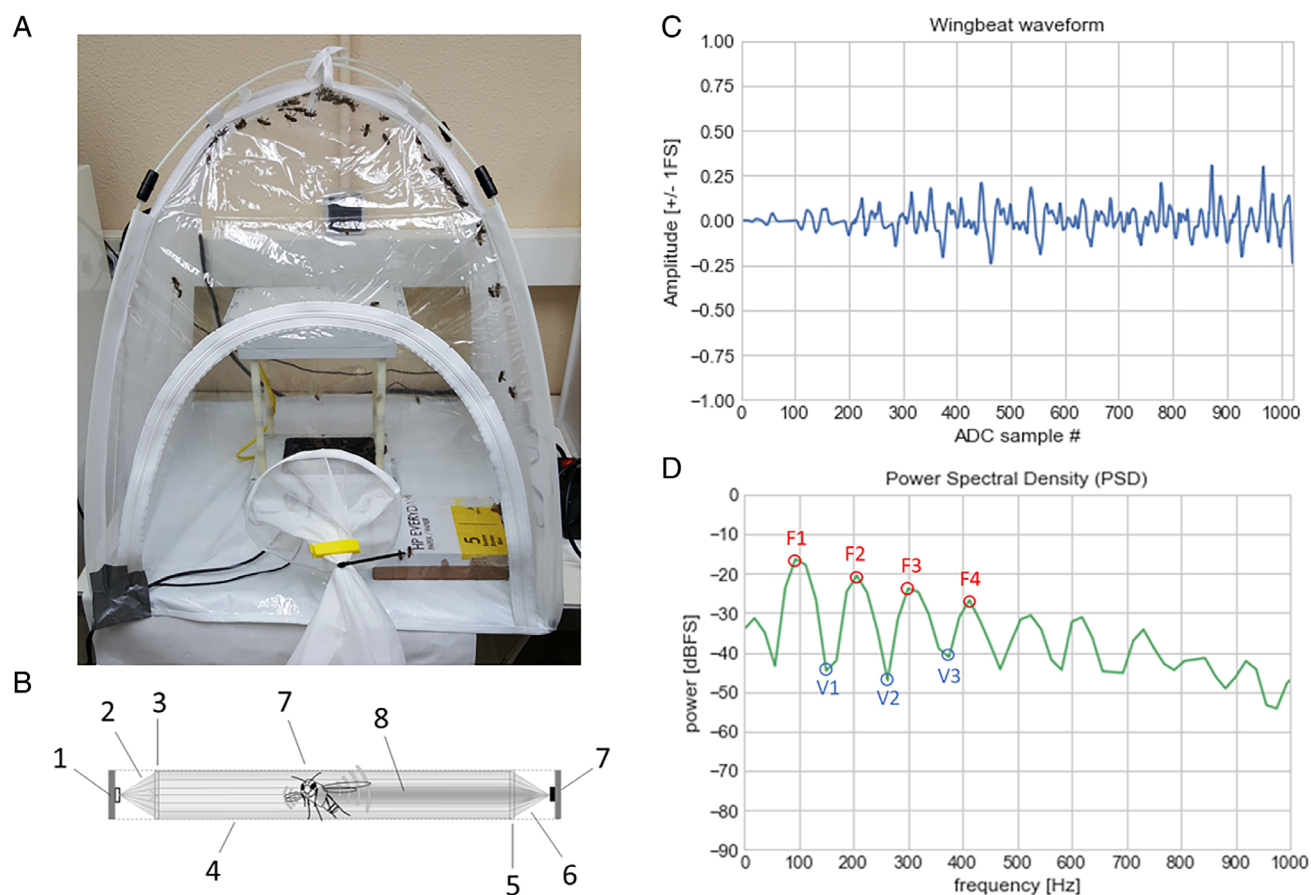
Figure 1. (A) Photo showing the optical sensor inside of the entomological tent. The optical sensor comprises an optical emitter module facing upwards and an optical receiver module facing downwards, with the modules separated by four white plastic posts, each with a length of 20 cm, such that insects may fly between the emitter and receiver modules. The black plastic cover on the emitter module is transparent to the infrared wavelengths used by the sensor. Beneath that cover is a 2D array of collimated optical emitters which project their light beams upwards towards the optical receiver module. The optical receiver module contains a 2D array of downward facing optical receivers also covered by black plastic which is not visible in the photo. The sensing volume is given by the 2D area common to both the emitter and receiver (71 cm^2) multiplied by the distance between the black plastic covers (19.4 cm). (B) illustrates the basic operation of each optical emitter-receiver in which a LED (1) emits a diverging beam of light (2), which falls upon a lens (3) that form a collimated beam of light (4), which after a certain distance, falls upon a second lens (5) that forms a converging beam (6), which focuses onto a photodiode (7). When an insect (7) flies through the collimated beam (4), it casts a shadow (8) upon the photodiode (7) *i.e.*, the sensor uses the so-called optical extinction mode of operation. As the insect flaps its wings within the collimated beam (4), the light falling on the photodiode (7) is modulated, allowing determination of various wingbeat features of the flying insect. In the sensor, 24 optical emitter-receiver pairs are used to cover the 2D area described. (C) Example of a recorded flight with the ADC sample number (0 to 1023) on the x-axis, and amplitude on the y-axis with a range of [−1, 1] which corresponds to the full-scale range of the analog to digital converter (ADC) used to digitize the analog output of the optical receiver. The low frequency signal which corresponds to the body of the insect is not visible in the waveform due to a high-pass filter in the sensor, which also attenuates the impact of ambient light and electronic offset voltages. (D) The power spectral density (PSD) plot for the recording shown in (B), with frequency (Hz) on the x-axis and power (dB) on the y-axis. The fundamental, 2nd harmonic, 3rd harmonic, and 4th harmonic peaks for this PSD plot are indicated as F1, F2, F3, F4 respectively, and the 1st, 2nd and 3rd valleys are indicated as V1, V2, V3 respectively.

recording was long enough to provide acceptable frequency resolution. Longer recording times would have increased the possibility of more than one insect being recorded simultaneously. The sensor automatically added a timestamp to each recording.

After each recording session, each wingbeat recording was downloaded from the sensor and processed using a Python script (Python version 3.7.9) written by Irideon to produce a playable audio (WAV) file from which a series of features were extracted by the same script. Figure 1(C) shows the plot for a typical *V. velutina* WAV file, by way of example. The WAV waveform is not very informative on its own but can be processed to yield more informative data as will be described. The complete dataset contains 935 recordings as shown in Table 1.

2.2 Feature extraction

Using the Python script, each WAV file recording was processed to extract its power spectral density (PSD). A PSD is the measure of the signal's power content *versus* frequency in which the measurable frequency range is segmented into a series of discrete ranges referred to as bins. PSDs are used in numerous applications including the analysis of vibration and noise.[41] Each PSD was calculated using Welch's method[42] with a segment length of 512 ADC samples and an overlap of 50% to give the power per bin from 0 Hz to 4801.5 Hz in 256 bins, with a bin width of 18.756 Hz. As part of Welch's method, a window function (Hann window) was applied to each segment to reduce spectral leakage (side lobes) in the PSD due to the segmentation. The window function minimized spectral leakage due to a recording being
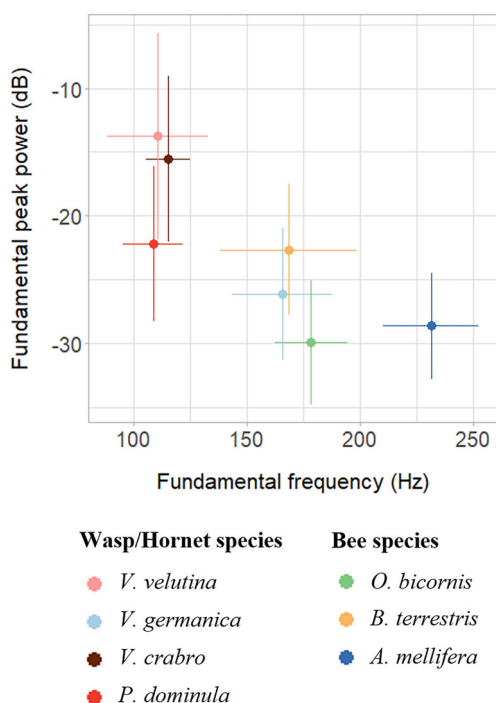
Figure 2. Mean fundamental frequency and fundamental peak power and standard deviation for the seven Hymenoptera species in this study.

terminated whilst the insect was still flying in the sensing volume. The powers in the PSD were corrected to compensate for the non-flat frequency response of the sensor and for insects which flew through the sensing zone before the end of the recording length (106.7 milliseconds). The PSD plot for a typical *V. velutina* recording is shown in Fig. 1(D).

From each PSD, the Python script extracted a series of machine learning features. A feature refers to an individual measurable property or characteristic extracted from a recording. The concept of feature is related to that of an explanatory variable used in statistical techniques. The features used in this work are illustrated in Fig. 1(D) and are described below.

(1) Wingbeat fundamental frequency in Hertz (Hz), referred to as F1 (Hz) was estimated using a combination of the following pitch determination methods[43]: autocorrelation, cepstrum and harmonic product spectrum. The wingbeat fundamental frequency is the frequency at which the insect flaps its wings. In cases where F1 (Hz) could not be determined with confidence, the recording was rejected from the data set.

(2) Fundamental peak power in decibels (dB) referred to as F1 (dB) is the power at F1 (Hz).

(3) A 14-value 'PSD peak and valley feature' comprising the frequencies and powers of the wingbeat fundamental frequency and the 2nd, 3rd, and 4th harmonics, and the frequencies and powers of the PSD valleys, which lie midway between each of the peaks, as depicted in Fig. 1(D). By definition, the harmonics frequencies are at integer (whole number) multiples of the fundamental frequency. The harmonic frequencies were estimated by calculating: $F2 = 2 \times F1$; $F3 = 3 \times F1$; and $F4 = 4 \times F1$. The PSD was then searched to find the maximum (peak) power within a small frequency range close to each of the estimated harmonic frequencies. The final values for each harmonic frequency were taken as the frequency at the corresponding peak power. The valley frequency and powers were calculated by searching the PSD for the minimum power (valley) approximately midway between the peaks on either side of the valley.

(4) A 2-value feature comprising only F1 (Hz) and F1 (dB).

(5) An 8-value feature comprising F1 (Hz) and the seven peak and valley powers, referred to as 'F1 (Hz) with peak and valley powers'.

2.3 Statistical analysis and classification of species using machine learning

For each species, the mean and standard deviation of the fundamental frequency and power were calculated to enable comparisons to be made. Differences in fundamental frequency and power between the seven species were assessed using a Kruskal–Wallis test and a Pairwise Wilcoxon Rank Sum Test with Holm adjustment, *post hoc*.

We also assessed the performance of a machine learning model to classify each of the seven Hymenopteran species using each of the five features described. The Random Forest machine learning algorithm with permutation parameter importance was used to develop the model. This algorithm generates multiple decision trees on a set of training data, each of them built over a random extraction of the observations from the dataset and a random extraction of the features, and the results obtained are combined in order to obtain a single model that is more robust and less prone to overfitting compared to the results of each tree separately.[44] The *ranger* package[45] implementation of the Random Forest algorithm was used.

We adopted a train-test split procedure, in which the dataset was divided into two subsets: the training set (70% of the full dataset) which was used to train the model; and the test set (the remaining 30% of the full dataset, and not used previously for training) which was used to evaluate the performance of the model, *i.e;* to determine how well the model classifies the species on new data. This procedure was repeated in 100 random train-test splits, which enables calculation of the mean and standard deviation of the performance metrics and of the feature importance.[44]

The performance of each model was evaluated using the following metrics: out-of-bag (OOB) error (estimated error resulting from the model prediction using the observations from the

Table 2. Mean classification accuracy (± standard deviation) for all species and for *V. velutina*, for the different features, indicating the number of PSD values comprising each feature

Feature	PSD values	Mean accuracy for all species	Accuracy for *V. velutina*
1 Fundamental frequency, F1 (Hz)	1	50.9 ± 20.9%	41.7 ± 8.0%
2 Fundamental peak power, F1 (dB)	1	27.2 ± 8.9%	43.4 ± 8.2%
3 PSD peak and valley feature	14	80.1 ± 13.9%	74.5 ± 7.0%
4 F1 (Hz) and F1 (dB)	2	60.0 ± 15.9%	58.4 ± 8.4%
5 F1 (Hz) with peak and valley powers (dB)	8	68.9 ± 13.8%	67.5 ± 8.4%

training set that are not used to create the trees)[44]; precision (proportion of correctly classified positives among all the samples classified as positive); recall (proportion of correctly classified positives among all the positives); f1 (which strikes a balance between precision and recall, in a single value metric)[46]; and accuracy (which describes the percentage of outcomes that the model has classified correctly). The equations for these metrics are:

$$Precision = \frac{TP}{TP+FP} \quad Recall = \frac{TP}{TP+FN} \quad f1 = 2 \cdot \frac{Precision \cdot Recall}{Precision + Recall}$$

$$Accuracy = \frac{TP+TN}{TP+TN+FP+FN}$$

Where TP (true positives) is the number of outcomes that the model correctly classifies as positive, TN (true negatives) is the number of outcomes that the model correctly classifies as
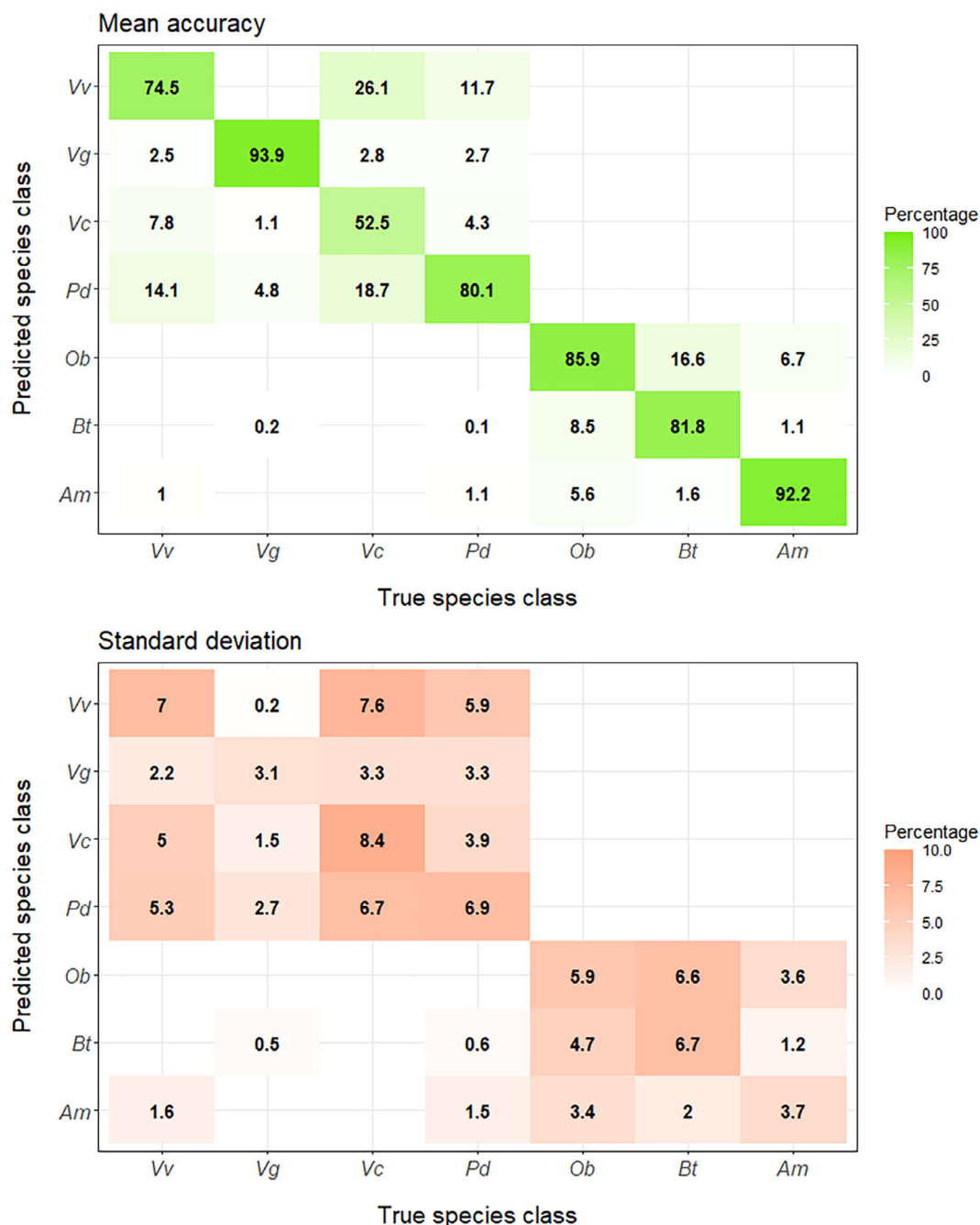
Figure 3. Confusion matrices assessing the performance of the machine learning model that predicts the identity of seven Hymenoptera species. The x-axes indicate the actual or 'true' species in the test set and the y-axes indicate the species predicted by the model. For each axis: *Vv* = *V. velutina*, *Vg* = *V. germanica*, *Vc* = *V. crabro*, *Pd* = *P. dominula*, *Ob* = *O. bicornis*, *Bt* = *B. terrestris*, *Am* = *A. mellifera*. In the upper plot, the value in each column indicates the percentage of samples in the true species (x-axis) which are classified into each of the predicted classes (y-axis). Consequently, each value on the diagonal, from the top left corner to the bottom right corner, indicates the percentage of samples in the class which is correctly classified. Values which do not lie on the diagonal indicate the percentage of confusion, or misclassification for the indicated classes. In the lower plot: the value in each cell indicates the standard deviation for the classification accuracy given in the corresponding cell of the upper plot. Zero values were removed for ease of visualization.

negative, FP (false positives) is the number of outcomes that the model incorrectly classifies as positive, and FN (false negatives) is the number of outcomes that the model incorrectly classifies as negative. All statistical analyses were performed with R (v4.0.2)[47] and statistical significance was set at $P < 0.05$.

3 RESULTS

The mean and standard deviation of the fundamental frequency and power for each species are shown in Fig. 2 (and are listed numerically in Supporting Information Tables S1 and S2). A high degree of overlap is apparent between *V. velutina*, *P. dominula* and *V. crabro* in one group, and between *V. germanica, B. terrestris* and *O. bicornis* in another. *A. mellifera* did not overlap with any of the other species studied. The standard deviations observed for each species indicate that the described methodology has yielded a reasonably rich and varied dataset for each.

V. velutina presented a fundamental frequency F1 (Hz) which was statistically lower than that of the other Hymenoptera species (Kruskal–Wallis $\chi^2 = 707.9$, df = 6, $P < 0.001$; Pairwise Wilcoxon Test, $P < 0.001$), except for *P. dominula* whose fundamental frequency was not significantly different to that of *V. velutina* (Pairwise Wilcoxon Test, $P = 0.7$). *V. velutina* also presented a fundamental power (F1 dB) which was statistically higher than those of the other Hymenoptera species (Kruskal–Wallis $\chi^2 = 462.63$, df = 6, $P < 0.001$; Pairwise Wilcoxon Test, $P < 0.05$).

The classification accuracy achieved using each of the different features is shown in Table 2. The highest accuracy for all species (80.1%) was achieved using the 14-value PSD peak and valley feature. The next highest accuracy (68.9%) was for the 8-value F1 (Hz) with peak and valley power feature. Consequently, under the conditions of this work, which includes the use of the Random Forest algorithm, the PSD harmonic and valley frequencies are seen to make a substantial contribution to model accuracy even though they are known to be highly correlated with F1 (Hz).

The performance of the machine learning model using the PSD peak and valley feature is considered good: OOB error = 16.9 ±

1.1%, Precision = 81.3 ± 2.5%, Recall = 80.1 ± 2.4% and f1 = 80.0 ± 2.5%.

The confusion matrices (Fig. 3) show the relationship between the true species identity and the species predicted by the trained model and includes the classification accuracy for each species. The highest classification accuracy was for *V. germanica* (93.9 ± 3.1%) and the lowest was for *V. crabro* (52.5 ± 8.4%). The accuracy for *V. velutina* was 74.5 ± 7.0% and the mean accuracy for all seven species was 80.1 ± 13.9%. Figure 3 indicates that *V. velutina* was mostly confused with *P. dominula*, and to a lesser degree with *V. crabro* and *V. germanica*. It also indicates that *V. crabro* was the species most often misclassified, confused mainly with *V. velutina* and *P. dominula*, which may be due to the relatively high overlap of the fundamental frequencies between these three species (Fig. 2). Figure 3. also shows a low rate of misclassification between *B. terrestris*, *O. bicornis* and *V. germanica* even though their fundamental frequency and power features are highly overlapped (Fig. 2). Figure 3 also indicates that the model shows very little confusion between the bee species and the wasp/hornet species.

All PSD peak and valley values made a positive contribution to the performance of the machine learning model (Fig. 4). The most important value was fundamental frequency F1 (Hz) and the next five most important values were also related to frequency. The most important power value was F1 (dB) which was in 7th place overall.

4 DISCUSSION

We recorded the flights from seven species of Hymenoptera, including *V. velutina*, using an optical sensor and extracted five wingbeat frequency and power features from the PSD of each recorded waveform. We performed a statistical analysis of the fundamental wingbeat frequency and power of each species. We also used the features in a machine learning model and assessed the performance of the model to classify each species.

There is good agreement between the wingbeat fundamental frequencies of our work and that of previous works for: *A. mellifera* (251 Hz),[25] *B. terrestris* (170 Hz),[48] *V. germanica*
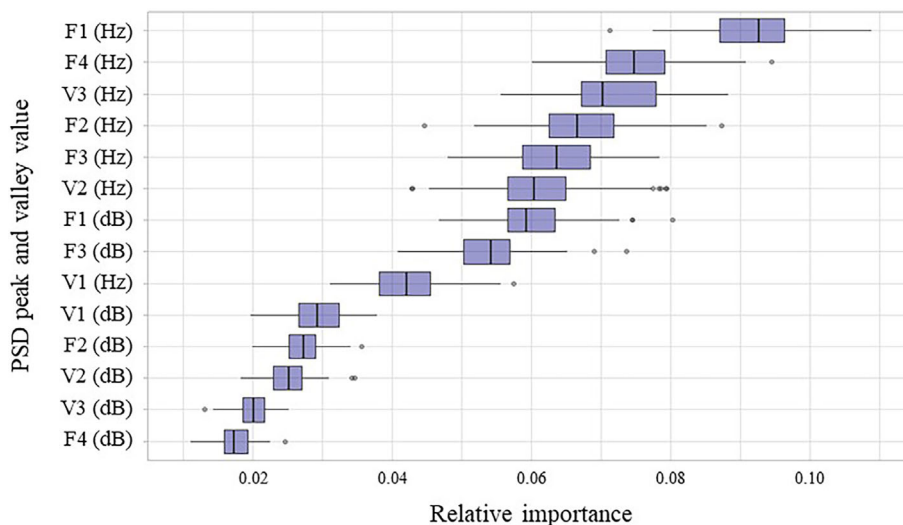
Figure 4. Box and whisker plots for the relative importance of each of the PSD peak and valley value. The boxes indicate the interquartile range (IQR) from Q1 to Q3. The vertical line within each box indicates the median. The horizontal lines show the 'minimum' to 'maximum' range, from Q1–1.5 × IQR to Q3 + 1.5 × IQR, with outliers shown as dots.

(148 Hz)[49] and other *Vespa* (*V. crabro* = 100 Hz; *V. simillima xanthoptera* = 100 Hz and *V. orientalis* = 125 Hz).[25,50,51] Our study was performed using insects flying in an entomological tent, which may have affected insect flight characteristics compared to natural flight in the field. However, the fundamental frequency we obtained for *A. mellifera* (231.5 ± 21.1 Hz) is similar to that reported in another work (251.2 Hz ± 45.0 Hz)[25] in which the recordings were made outdoors in a rural area. To the best of our knowledge, the present work is the first to report the wingbeat frequencies of *V. velutina*, *P. dominula*, and *O. bicornis*.

Previous studies have shown that Hymenoptera wingbeat frequencies are generally inversely proportional to body size (which depends on caste and sex)[52,53] and to wing length.[48,54] This is consistent with our findings, in which the lowest fundamental frequencies correspond to *V. velutina* and *V. crabro* which are predators of insects and are larger than bees.[25]

In the present work, we assessed classification performance using frequency and power values from the PSD in addition to fundamental frequency. The 14-value peak and valley feature gave the best classification performance, which was 80.1 ± 13.9% on average for all species and 74.5 ± 7.0% for *V. velutina*. Other studies show comparable accuracy results for the classification of Hymenoptera species (Gradišek *et al.*[52] = 82.7%; Kawakita & Ichikawa[25] = 85.3%), and for other insects, such as mosquitoes (Fernandes *et al.*[46] = 78.1%).

Wingbeat fundamental frequency is the feature most used in works pertaining to insect species classification using audio recordings[25,39] with wingbeat harmonics used to a lesser extent.[55,56] In the present work, wingbeat fundamental frequency F1 (Hz) was found to be the most important single-value feature.

Previous studies have also assessed other features as an alternative to, or in combination with wingbeat fundamental frequency. For example, Eyben, Wöllmer, and Schuller[57] provide a feature extraction tool (openSMILE) for audio analysis, which was used by Gradišek *et al.*[52] to compute 1582 numerical features for bumblebee species classification. Features studied in comparable species classification works include minimum and maximum frequencies[23]; maximum power[23]; frequency and power modulations[58]; full spectrogram[46,59]; raw waveforms[59]; spectrum octave analysis[22]; and wingbeat harmonics.[55,56]

In this study, only a relatively small dataset was available to train and test the machine learning model, but it was large enough to achieve good levels of classification accuracy. To further improve model performance, planned future work includes collecting and recording more insects to increase the size of the dataset and to improve the numeric balance within the species, caste, and sex classes. Consideration of wingbeat frequency and recording time stamp could be made to provide a rough indicator of individual insects which fly though the open sensor multiple times.

The results of the present work indicate potential for the development of an automated system to monitor populations of *V. velutina* in the field to assist localized management actions and provide information about the ecology of the species to better understand its spatio-temporal patterns across environmental gradients. Classification accuracy for *V. velutina* would probably be higher than 74.5% if a sensor were placed in an apiary since there would be no confusion of *V. velutina* with *A. mellifera*. Nevertheless, the presence of *P. dominula* or *V. crabro* could result in reduced accuracy in localities where they coexists with *V. velutina*.

A range of attractants could be considered for use with the sensor in the field, to attract target insects towards the sensor, where needed. Potential recruitment substances for *V. velutina* include baits which have been tested with that species[9,60] and hive products, protein sources, and chemical substances.[61] Likewise, a sex pheromone for attracting *V. velutina* males has been identified, which could be used to attract males in autumn[62] although it is not yet available for field use.

Furthermore, given that Hymenoptera wingbeat frequency is generally inversely proportional to insect age[63]; and is a strong indicator of insect rate of metabolism and physical structure[64]; and changes during bumblebee buzz pollination,[53] it might be possible to develop new machine learning models for the optical sensor to classify such attributes and behavior, in addition to species. In addition, differences in wing shape have been found between haploid and diploid males in *B. terrestris*.[65] As such, it would be interesting to determine if there are differences in wing shape between haploid and diploid males of *V. velutina* which may be detectable using the sensor. This could be of interest in an integrated invasive alien species management program because, in Europe, diploid males of *V. velutina* are sterile and haploid males are fertile.[66]

The present study could be a first step in multiple avenues of research, with potential application of the sensor in the field with machine learning models for automated monitoring of the biodiversity of Hymenoptera and possibly insects in other orders, and the monitoring of flying invasive alien and pest species. A further potential application could be in the agro-food industry to monitor pollination performed by bees and other pollinating insects.

5 CONCLUSIONS

Our study demonstrates the effectiveness of the optical sensor and machine learning methods to identify seven common hymenopteran species which demonstrated an average classification accuracy of 80.1 ± 13.9% and an accuracy of 74.5 ± 7.0% for the invasive alien *V. velutina*, which was the primary target species for this work. The insects were collected in the field and recorded in an entomological tent in the laboratory. We conclude that the approach shows promise for the development of a system for automatic detection of the invasive *V. velutina* in the field, in the presence of common wasp and bee species.

AUTHORS' CONTRIBUTIONS

CH, MW, JE and ML conceived the ideas and designed methodology. CH collected, analyzed the data and led the writing of the manuscript. MW, JE, NRP, BF, JAJR and ML contributed critically to the draft. All authors gave final approval for publication.

CONFLICT OF INTEREST STATEMENT

There are no conflicts to declare regarding the contents of this publication.

Pest Manag Sci 2023; **79**: 1225–1233 · · · © 2022 The Authors. · · · wileyonlinelibrary.com/journal/ps

Pest Management Science published by John Wiley & Sons Ltd on behalf of Society of Chemical Industry.

1231

DATA AVAILABILITY STATEMENT

The data that support the findings of this study are available from the corresponding author upon reasonable request.

SUPPORTING INFORMATION

Supporting information may be found in the online version of this article.

REFERENCES

1 Laurino D, Lioy S, Carisio L, Manino A and Porporato M, *Vespa velutina*: an alien driver of honey bee colony losses. *Diversity* **12**:1–15 (2020).
2 Barbet-Massin M, Salles JM and Courchamp F, The economic cost of control of the invasive yellow-legged Asian hornet. *NeoBiota* **55**: 11–25 (2020).
3 Monceau K, Bonnard O and Thiéry D, *Vespa velutina*: a new invasive predator of honeybees in Europe. *J Pest Sci* **2004**:1–16 (2014).
4 Leza M, Herrera C, Marques A, Roca P, Sastre-Serra J and Pons DG, The impact of the invasive species *Vespa velutina* on honeybees: a new approach based on oxidative stress. *Sci Total Environ* **689**:709–715 (2019).
5 Rojas-Nossa SV and Calviño-Cancela M, The invasive hornet *Vespa velutina* affects pollination of a wild plant through changes in abundance and behaviour of floral visitors. *Biol Invasions* **22**:2609–2618 (2020).
6 Reaser JK, Burgiel SW, Kirkey J, Brantley KA, Veatch SD and Burgos-Rodríguez J, The early detection of and rapid response (EDRR) to invasive species: a conceptual framework and federal capacities assessment. *Biol Invasions* **22**:1–19 (2020).
7 Monceau K, Bonnard O and Thiéry D, Chasing the queens of the alien predator of honeybees: a water drop in the invasiveness ocean. *Open J Ecol* **02**:183–191 (2012).
8 Leza M, Herrera C, Picó G, Morro T and Colomar V, Six years of controlling the invasive species *Vespa velutina* in a Mediterranean Island: the promising results of an eradication plan. *Pest Manage Sci* **77**: 2375–2384 (2021).
9 Rojas-Nossa SV, Novoa N, Serrano A and Calviño-Cancela M, Performance of baited traps used as control tools for the invasive hornet *Vespa velutina* and their impact on non-target insects. *Apidologie* **49**:872–885 (2018).
10 Rodríguez-Flores MS, Seijo-Rodríguez A, Escuredo O and Seijo-Coello M d C, Spreading of *Vespa velutina* in northwestern Spain: influence of elevation and meteorological factors and effect of bait trapping on target and non-target living organisms. *J Pest Sci* **92**: 557–565 (2004) Springer Berlin Heidelberg (2019).
11 Kennedy PJ, Ford SM, Poidatz J, Thiéry D and Osborne JL, Searching for nests of the invasive Asian hornet (*Vespa velutina*) using radio-telemetry. *Commun Biol* **1**:1–8 (2018).
12 Maggiora R, Saccani M, Milanesio D and Porporato M, An innovative harmonic radar to track flying insects: the case of *Vespa velutina*. *Sci Rep* **9**:1–10 (2019).
13 Lioy S, Bianchi E, Biglia A, Bessone M, Laurino D and Porporato M, Viability of thermal imaging in detecting nests of the invasive hornet *Vespa velutina*. *Insect Sci* **28**:271–277 (2021).
14 Reynaud L and Guérin-Lassous I, Design of a force-based controlled mobility on aerial vehicles for pest management. *Ad Hoc Networks* **53**:41–52 (2016).
15 Sakata MK, Watanabe T, Maki N, Ikeda K, Kosuge T, Okada H *et al.*, Determining an effective sampling method for eDNA metabarcoding: a case study for fish biodiversity monitoring in a small, natural river. *Limnology* **22**:221–235 (2021).
16 Weiskopf SR, McCarthy KP, Tessler M, Rahman HA, McCarthy JL, Hersch R *et al.*, Using terrestrial haematophagous leeches to enhance tropical biodiversity monitoring programmes in Bangladesh. *J Appl Ecol* **55**:2071–2081 (2018).
17 Rocchini D, Luque S, Pettorelli N, Bastin L, Doktor D, Faedi N *et al.*, Measuring *β*-diversity by remote sensing: a challenge for biodiversity monitoring. *Methods Ecol Evol* **9**:1787–1798 (2018).
18 Carvalho J, Hipólito D, Santarém F, Martins R, Gomes A, Carmo P *et al.*, Patterns of *Vespa velutina* invasion in Portugal using crowdsourced data. *Insect Conserv Diversity* **13**:501–507 (2020).
19 Buxton RT, McKenna MF, Clapp M, Meyer E, Stabenau E, Angeloni LM *et al.*, Efficacy of extracting indices from large-scale acoustic recordings to monitor biodiversity. *Conserv Biol* **32**:1174–1184 (2018).
20 Blumstein DT, Mennill DJ, Clemins P, Girod L, Yao K, Patricelli G *et al.*, Acoustic monitoring in terrestrial environments using microphone arrays: applications, technological considerations and prospectus. *J Appl Ecol* **48**:758–767 (2011).
21 Potamitis I, Classifying insects on the fly. *Ecol Inf* **21**:40–49 (2014).
22 González-Hernández FR, Sánchez-Fernández LP, Suárez-Guerra S and Sánchez-Pérez LA, Marine mammal sound classification based on a parallel recognition model and octave analysis. *Appl Acoust* **119**: 17–28 (2017).
23 Acevedo MA, Corrada-Bravo CJ, Corrada-Bravo H, Villanueva-Rivera LJ and Aide TM, Automated classification of bird and amphibian calls using machine learning: a comparison of methods. *Ecol Inf* **4**:206–214 (2009).
24 Khalighifar A, Brown RM, Goyes Vallejos J and Peterson AT, Deep learning improves acoustic biodiversity monitoring and new candidate forest frog species identification (genus *Platymantis*) in The Philippines. *Biodivers Conserv* **30**:643–657 (2021).
25 Kawakita S and Ichikawa K, Automated classification of bees and hornet using acoustic analysis of their flight sounds. *Apidologie* **50**: 71–79 (2019).
26 Khalighifar A, Komp E, Ramsey JM, Gurgel-Gonçalves R and Peterson AT, Deep learning algorithms improve automated identification of Chagas disease vectors. *J Med Entomol* **56**:1404–1410 (2019).
27 Towsey M, Wimmer J, Williamson I and Roe P, The use of acoustic indices to determine avian species richness in audio-recordings of the environment. *Ecol Inf* **21**:110–119 (2014).
28 Celis-Murillo A, Deppe JL and Allen MF, Using soundscape recordings to estimate bird species abundance, richness, and composition. *J Field Ornithol* **80**:64–78 (2009).
29 Farina A, Pieretti N and Morganti N, Acoustic patterns of an invasive species: the red-billed Leiothrix (*Leiothrix lutea* Scopoli 1786) in a Mediterranean shrubland. *Bioacoustics* **22**:175–194 (2013).
30 Hu W, Bulusu N, Chou CT, Jha S, Taylor A and Tran VN, Design and evaluation of a hybrid sensor network for cane toad monitoring. *ACM Trans Sens Networks* **5**:1–28 (2009).
31 Mankin RW and Moore A, Acoustic detection of *Oryctes rhinoceros* (Coleoptera: Scarabaeidae: Dynastinae) and *Nasutitermes luzonicus* (Isoptera: Termitidae) in palm trees in urban Guam. *J Econ Entomol* **103**:1135–1143 (2010).
32 Potamitis I, Ganchev T and Kontodimas D, On automatic bioacoustic detection of pests: the cases of *Rhynchophorus ferrugineus* and *Sitophilus oryzae*. *J Econ Entomol* **102**:1681–1690 (2009).
33 Balestrino F, Iyaloo DP, Elahee KB, Bheecarry A, Campedelli F, Carrieri M *et al.*, A sound trap for *Aedes albopictus* (Skuse) male surveillance: response analysis to acoustic and visual stimuli. *Acta Trop* **164**: 448–454 (2016).
34 Li Y, Zilli D, Chan H, Kiskin I, Sinka M, Roberts S *et al.*, Mosquito detection with low-cost smartphones: data acquisition for malaria research. *arXiv* 1–5 (2017).
35 Mukundarajan H, Hol FJH, Castillo EA, Newby C and Prakash M, Using mobile phones as acoustic sensors for high-throughput mosquito surveillance. *Elife* **6**:1–26 (2017).
36 Brydegaard M, Towards quantitative optical cross sections in entomological laser radar - potential of temporal and spherical parameterizations for identifying atmospheric fauna. *PLoS One* **10**:1–15 (2015).
37 Kirkeby C, Wellenreuther M and Brydegaard M, Observations of movement dynamics of flying insects using high resolution lidar. *Sci Rep* **6**: 1–11 (2016).
38 Mullen ER, Rutschman P, Pegram N, Patt JM, Adamczyk JJ and Johanson E, Laser system for identification, tracking, and control of flying insects. *Opt Express* **24**:11828–11838 (2016).
39 González-Pérez MI, Faulhaber B, Williams M, Brosa J, Aranda C, Pujol N *et al.*, A novel optical sensor system for the automatic classification of mosquitoes by genus and sex with high levels of accuracy. *Parasites Vectors* **15**:1–11, BioMed Central (2022).
40 Utility Model 202000562, Boletín Oficial de la Propiedad Industrial Num. 5904, ISSN: 1889–1292, NIPO: 088170165, 30/4/2021 (2021).
41 Norton MP and Karczub DG, *The Analysis of Noise and Vibration Signals, Fundamentals of Noise and Vibration Analysis for Engineers*. Cambridge University Press, Cambridge, pp. 342–382 (2003).

42 Villwock S and Pacas M, Application of the Welch-method for the identification of two- and three-mass-systems. *IEEE Trans Ind Electron* **55**: 457–466 (2008).

43 Cai W, *Analysis of Acoustic Feature Extraction Algorithms in Noisy Environments*. University of Rochester, New York (2013).

44 Breiman L, Random forests. *Mach Learn* **45**:5–32 (2001).

45 Wright MN and Ziegler A, Ranger: a fast implementation of random forests for high dimensional data in C++ and R. *J Stat Softw* **77**:1–17 (2017).

46 Fernandes MS, Cordeiro W and Recamonde-Mendoza M, Detecting *Aedes aegypti* mosquitoes through audio classification with convolutional neural networks. *Comput Biol Med* **129**:104152 (2021).

47 RStudio Team, *RStudio: Integrated Development for R*. RStudio, PBC, Boston, MA (2020).

48 van Roy J, De Baerdemaeker J, Saeys W and De Ketelaere B, Optical identification of bumblebee species: effect of morphology on wingbeat frequency. *Comput Electron Agric* **109**:94–100 (2014).

49 Tercel MPTG, Veronesi F and Pope TW, Phylogenetic clustering of wingbeat frequency and flight-associated morphometrics across insect orders. *Physiol Entomol* **43**:149–157 (2018).

50 Ishay J, Frequencies of the sounds produced by the oriental hornet, Vespa orientalis. *J Insect Physiol* **21**:1737–1740 (1975).

51 Byrne BYDN, Buchmann SL and Spangler HG, Relationship between wing loading, wingbeat frequency and body mass in homopterous insects. *J Exp Biol* **135**:9–23 (1998).

52 Gradišek A, Slapničar G, Šorn J, Luštrek M, Gams M and Grad J, Predicting species identity of bumblebees through analysis of flight buzzing sounds. *Bioacoustics* **26**:63–76 (2016).

53 Burkart A, Lunau K and Schlindwein C, Comparative bioacoustical studies on flight and buzzing of neotropical bees. *J Pollination Ecol* **6**: 118–124 (2012).

54 Miller-Struttmann NE, Heise D, Schul J, Geib JC and Galen C, Flight of the bumble bee: buzzes predict pollination services. *PLoS One* **12**: 1–14 (2017).

55 Raman DR, Gerhardt RR and Wilkerson JB, Detecting insect flight sounds in the field: implications for acoustical counting of mosquitoes. *Trans ASABE* **50**:1481–1485 (2007).

56 Cator LJ, Arthur BJ, Harrington LC and Hoy RR, Harmonic convergence in the love songs of the dengue vector mosquito. *Science* **80**:1077–1079 (2009).

57 Eyben F, Wöllmer M and Schuller B, OpenSMILE - the Munich versatile and fast open-source audio feature extractor. *MM'10 - Proc ACM Multimed 2010 Int Conf*:1459–1462 (2010).

58 Arthur BJ, Emr KS, Wyttenbach RA and Hoy RR, Mosquito (*Aedes aegypti*) flight tones: frequency, harmonicity, spherical spreading, and phase relationships. *J Acoust Soc Am* **135**:933–941 (2014).

59 Becker S, Ackermann M, Lapuschkin S, Müller K-R and Samek W, Interpreting and explaining deep neural networks for classification of audio signals. *arXiv*:2–6 (2018).

60 Lioy S, Laurino D, Capello M, Romano A, Manino A and Porporato M, Effectiveness and selectiveness of traps and baits for catching the invasive hornet *Vespa velutina*. *Insects* **11**:1–13 (2020).

61 Couto A, Monceau K, Bonnard O, Thiéry D and Sandoz JC, Olfactory attraction of the hornet *Vespa velutina* to honeybee colony odors and pheromones. *PLoS One* **9**:1–19 (2014).

62 Wen P, Cheng Y-N, Dong S-H, Wang Z-W, Tan K and Nieh JC, The sex pheromone of a globally invasive honey bee predator, the Asian eusocial hornet, Vespa velutina. *Sci Rep* **7**:1–11 (2017).

63 Parmezan ARS, Souza VMA, Žliobaitė I and Batista GEAPA, Changes in the wing-beat frequency of bees and wasps depending on environmental conditions: a study with optical sensors. *Apidologie* **52**:731–748 (2021).

64 Santoyo J, Azarcoya W, Valencia M, Torres A and Salas J, Frequency analysis of a bumblebee (*Bombus impatiens*) wingbeat. *Pattern Anal Appl* **19**:487–493 (2016).

65 Bortolotti L, Fiorillo F, Dall'Olio R, Cejas D, De la Rúa P and Bogo G, Ploidy determination in *Bombus terrestris* males: cost-efficiency comparison among different techniques. *J Apic Res* **61**:180–189, Taylor & Francis (2022).

66 Darrouzet E, Gévar J, Guignard Q and Aron S, Production of early diploid males by European colonies of the invasive hornet *Vespa velutina nigrithorax*. *PLoS One* **10**:1–9 (2015).